1-1-2013

Smaller, faster stomata: scaling of stomatal size, rate of response, and stomatal conductance

Paul Drake

Raymond H. Froend
Edith Cowan University

Peter Franks

10.1093/jxb/ers347

This is a pre-copyedited, author-produced PDF of an article accepted for publication in Journal Of Experimental Botany, *following peer review. The version of record* Drake, P., Froend, R. H., & Franks, P. (2013). Smaller, faster stomata: scaling of stomatal size, rate of response, and stomatal conductance. Journal Of Experimental Botany, 64(2), 495-505, *is available online here.*

Smaller, faster stomata: Scaling of stomatal size, rate of response and stomatal conductance

Paul L. Drake[1], Ray H. Froend[2] and Peter J. Franks[3]

[1]Natural Resources Branch, Department of Environment and Conservation, Locked Bag 104, Bentley Delivery Centre, WA 6983, Australia

[2]School of Natural Sciences, Edith Cowan University, 270 Joondalup Drive, Joondalup, WA 6027, Australia 6027

[3]Faculty of Agriculture and Environment, University of Sydney, Sydney, NSW 2006

Author for correspondence: Peter Franks

Phone: +61 2 8627 1051
Fax: +61 2 8627 1099

Email: peter.franks@sydney.edu.au

Running title: Scaling of stomatal traits

Words: 3, 913 (body)

Tables: 2

Figures: 9

ABSTRACT

Maximum and minimum stomatal conductance, as well as stomatal size and rate of response, are known to vary widely across plant species, but the functional relationship between these static and dynamic stomatal properties is unknown. Our objective was to test three hypotheses: (i) operating stomatal conductance under standard conditions (g_{op}) correlates with minimum stomatal conductance prior to morning light, ($g_{min(dawn)}$); (ii) stomatal size (S) is negatively correlated with g_{op} and the maximum rate of stomatal opening in response to light , $(dg/dt)_{max}$; (iii) g_{op} correlates negatively with instantaneous water-use efficiency (WUE) despite positive correlations with maximum rate of carboxylation (V_{cmax}) and light-saturated rate of electron-transport (J_{max}). Using five closely related species of the genus *Banksia*, we measured the above variables and found that all three hypotheses were supported by the results. Overall, this suggests that leaves built for higher rates of gas exchange have smaller stomata and faster dynamic characteristics. With the aid of a stomatal control model we demonstrate that higher g_{op} can potentially expose plants to larger tissue water potential gradients, and that faster stomatal response times can help offset this risk.

Key words: stomatal size, maximum stomatal conductance, night-time conductance, transpiration, stomatal control, water-use efficiency

INTRODUCTION

Plants regulate stomatal conductance to optimise carbon uptake with respect to water loss (Cowan, 1977; Farquhar *et al*., 1980). An important limitation in this process is the rate at which stomata open in the light or close under darkness or water deficit (Cowan, 1977; Hetherington and Woodward 2003; Franks and Farquhar 2007; Brodribb *et al*., 2009; Lawson *et al*., 2011, Vico *et al*., 2011). However, although stomatal response times are known to vary widely across species (Assmann and Grantz 1990; Franks and Farquhar 2007; Vico *et al*., 2011), the biophysical factors governing the rate of response are not well understood.

Plant photosynthetic productivity and water-use efficiency also are linked to the dynamic range of stomatal conductance. Under favourable conditions of low evaporative demand and high light, productivity is constrained by the maximum operating stomatal conductance, g_{op}, and under severe water deficits resulting from high evaporative demand and/or dry soil, plants rely upon full stomatal closure and a highly water-impermeable leaf cuticle to minimise water loss (Hinckley *et al*., 1980; McDowell *et al*., 2008). Across plant taxa there is a wide range of operating and minimum stomatal conductances (Jones, 1992; Schulze *et al*., 1994; Körner, 1995). However, it is not known if maximum and minimum stomatal conductance typically scale with one another.

Commonly defined as the minimum stomatal conductance in darkness, g_{min} for a given leaf may differ on account of the time of day or other physiological circumstances. For example, stomata typically close in response to darkness and remain so for much of the night, but often the closure is not complete. In fact the night-time or 'nocturnal' conductance can be sufficient to allow significant transpiration (Ehrler, 1971; Benyon, 1999; Snyder, *et al*, 2003; Barbour *et al*., 2005; Bucci *et al*., 2005; Daley and Phillips, 2006; Dawson *et al*., 2007), and growth conditions may produce stomata that cannot close completely even when fully deflated at zero turgor (Franks and Farquhar, 2007). Night-time transpiration rates are typically between 5% to 15% of daytime transpiration, but in rare cases can be more than 30% (Caird *et al*., 2007; Novick *et al*., 2009). Such high rates of water loss at times of little or no carbon gain are inconsistent with the general role of stomata as a water conserving apparatus, but little is known about the mechanism of nocturnally elevated stomatal conductance or its relationship to the minimum conductance in

darkness at other times of the day and under desiccation. Here we distinguish between three different conductance minima according to the circumstances in which they are promoted: (i) $g_{min(dawn)}$, referring to the minimum stomatal conductance to water vapour at the end of the nocturnal dark phase; (ii) $g_{min(day)}$, referring to the minimum stomatal conductance to water vapour attained when the leaf is exposed to a period of darkness during to normal daylight hours; (iii) the absolute minimum conductance to water vapour, $g_{min(abs)}$, occurring when the guard cells are fully deflated as a result of complete turgor loss (Fig. 1). The quantities g_{op}, $g_{min(dawn)}$, $g_{min(day)}$, and $g_{min(abs)}$ all comprise a stomatal component in parallel with a cuticular component, although $g_{min(abs)}$ may closely approximate cuticular conductance. Common empirical stomatal models do not adequately account for elevated minimum conductance at night or its environmental sensitivities (Barbour and Buckley, 2007) but few studies have measured all of these conductances together so the relationship between them is obscure.

The operating stomatal conductance, g_{op}, is also known to scale with other leaf gas exchange and water transport attributes, such as CO_2 assimilation rate and leaf hydraulic conductance (Meinzer, 2003; Brodribb *et al*., 2007). However, nonlinearities in some of these relationships result in trade-offs. For example, increased CO_2 assimilation rate accompanying higher g_{op} may be associated with lower water-use efficiency (Franks and Farquhar, 1999) and higher leaf water potential gradients (Franks, 2006). Improved stomatal dynamic properties with increased g_{op} could potentially help to offset these counterproductive properties.

The operating conductance g_{op} is constrained by the maximum stomatal conductance, g_{max}, which in turn is determined by two physical attributes of stomata, (i) their size (S) and (ii) their density (D), or number per unit area. We distinguish between g_{max} and g_{op} because g_{max} relates to stomata opened to their widest possible apertures (e.g. under 100% relative humidity and low ambient CO_2 concentration), whereas under typical operating conditions (less than 100% relative humidity and normal ambient CO_2 concentration) stomatal apertures will be less than fully open. It has been shown that across broad geological timescales and evolutionary lineages higher g_{max} and g_{op} are associated with smaller stomatal size and higher density, and that S is negatively correlated with D (Hetherington and Woodward, 2003; Franks and Beerling, 2009). This relationship has also been found to apply within a single species across environmental gradients (Franks *et al*., 2009), and also across a group

of six tree species of different genus (Aasama *et al*., 2001). Smaller stomata, due to their greater membrane surface are to volume ratio, may have faster response times compared to larger stomata, and this in combination with high stomatal density may allows the leaf to attain high g_{op} rapidly under favorable conditions, and to rapidly reduce conductance when conditions are unfavorable. In such a system, the rate of stomatal response would be positively correlated with g_{op} and negatively correlated stomatal size. However, to date, these functional relationships have not been confirmed.

Our objective was to test three hypotheses: (i) operating stomatal conductance under standard conditions (g_{op}) correlates with minimum stomatal conductance prior to morning light, ($g_{min(dawn)}$); (ii) stomatal size (S) is negatively correlated with g_{op} and the maximum rate of stomatal opening in response to light , $(dg/dt)_{max}$; (iii) g_{op} correlates negatively with instantaneous water-use efficiency (WUE) despite positive correlations with maximum rate of carboxylation (V_{cmax}) and light-saturated rate of electron-transport (J_{max}). To test our hypotheses we measured the above traits in a closely related group of *Banksia* species that are distributed across a broad hydrological environment from wetlands to dune crests (Fig. 2) (Groom, 2002; Groom, 2004). Restricting the study to a single genus ensured minimal genetic variability while offering a broad range of g_{op}, stomatal size and stomatal density traits for analysis. The results are assessed in terms of their implications for plant water balance and fitness under the differing hydrological habitats of the study species.

MATERIALS AND METHODS

Plant material

Five *Banksia* species, endemic to the *Banksia* woodland of south-western Australia (31°45’ S, 115°57’ E), were selected for study. The species were as follow: *Banksia attenuata* R.Br., *Banksia menziesii* R.Br., *Banksia ilicifolia* R.Br., *Banksia prionotes* Lindl. and *Banksia littoralis* R.Br. Figure 2, based on the natural geographical range of south-west Australian banksias, is an idealised representation of the distribution of the species across five distinct habitats as defined by the depth of groundwater from the natural surface (Table 1).

Four plants from each species were grown from seed in a glasshouse in 10 L pots. Plants were allowed to develop in 70:30 coarse sand:humus and fertilized with 33.38 ± 0.24 grams (mean ± SE) of slow release fertilizer (Osmocote™). All plants were well watered throughout development and maintained under a day/night temperature regime of 24/15°C. When leaves had fully matured under these conditions, each plant was periodically transferred to a laboratory (air temperature range = 23 ± 3°C), rewatered and allowed to equilibrate overnight in preparation for the following day's gas exchange measurements.

Gas exchange

Leaf gas exchange properties were measured in the laboratory with an open-flow portable photosynthesis system (Model Li 6400, Li-cor Inc, Lincoln, Nebraska) on one leaf per plant (n = 4 plants per species). All experiments were initiated early in the morning (07:30 – 08:30 local standard time) and were concluded within the natural daylight photoperiod. Plants were kept well watered throughout measurements. Measurements were made on fully expanded leaves (three or four leaves back from a branch apex). Throughout experiments the ambient mole fraction of CO_2 (c_a) was maintained at 350 μmol CO_2 mol^{-1} air (except for relationships between assimilation rate (A) and intercellular mole fraction of CO_2 (c_i)), leaf temperature was set at 20°C and leaf-to-air vapour pressure difference regulated to 1 kPa.

In the morning, minimum steady-state stomatal conductance to water vapour prior to light exposure ($g_{min(dawn)}$, mol H_2O m^{-2} leaf s^{-1}) was determined with the leaf in darkness. A stomatal opening phase, comprising the transition from $g_{min(dawn)}$ to a maximum steady-state or operating stomatal conductance to water vapour (g_{op}, mol H_2O m^{-2} leaf s^{-1}), was then recorded by exposing leaves to a photosynthetically active radiation (PAR) of 1500 μmol m^{-2} s^{-1} (while keeping the other chamber conditions constant) and logging instantaneous stomatal conductance (g) at 60 second intervals. This opening phase took approximately 120 minutes to reach a steady-state g_{op} for each species. After ensuring that all transient stomatal opening had ceased, the maximum steady-state CO_2 assimilation rate (A_{op}, μmol m^{-2} leaf s^{-1}) and corresponding intercellular CO_2 mole fraction ($c_{i\,(op)}$, μmol CO_2 mol^{-1} air) and steady-

state transpiration rate (E_{op}, mmol H_2O m^{-2} leaf s^{-1}) were also recorded. Also at this point, the relationship between instantaneous CO_2 assimilation rate A and leaf intercellular CO_2 concentration c_i was obtained (see below). Photosynthetically active radiation was then returned to zero and the subsequent stomatal closing phase, to a minimum steady-state value, $g_{min(day)}$, was recorded by logging stomatal conductance at 60 second intervals. The timeframe for stomatal closure varied across species, ranging from approximately 100 to 250 minutes. The leaf was then excised from the plant and any further decline in stomatal conductance recorded, with the final minimum conductance for excised leaves measured as the absolute minimum, $g_{min(abs)}$.

The relationship between A and c_i was obtained for each plant by manipulating c_a over the range 50 μmol CO_2 mol^{-1} air to 2000 μmol CO_2 mol^{-1} air, beginning with the steady state conditions at 350 μmol CO_2 mol^{-1} air, then stepping c_a down to 300, 200, 100, 50 and then up to 400, 600, 800, 1000, 1400, 1800 and 2000 μmol CO_2 mol^{-1} air. We characterised the relationship according to the model proposed by Farquhar *et al*. (1980) and subsequently modified by von Caemmerer and Farquhar (1981), Sharkey (1985) and Harley *et al*. (1992). Undertaking this mechanistic analysis of the relationship between A and c_i yielded estimates for the maximum rate of carboxylation (Vc_{max}, μmol CO_2 m^{-2} leaf s^{-1}) and the light saturated rate of electron transport (J_{max}, μmol CO_2 m^{-2} leaf s^{-1}).

Deriving the maximum rate of stomatal opening

Plots of instantaneous stomatal conductance (g) versus time elapsed since the start of measurements (t, seconds) obtained during the stomatal opening phase were described by Boltzmann sigmoidal models:

$$g = \frac{a_1 - a_2}{1 + e^{t - t_0/dt'}} + a_2 \quad (1)$$

where a_1 (mol m^{-2} s^{-1}) is the left horizontal asymptote, a_2 (mol m^{-2} s^{-1}) is the right horizontal asymptote, t_0 (seconds) is the point of inflection and dt' (seconds) is the change in time that corresponds to the greatest change in g. Using an iterative least

squares fit approach, values for a_1, a_2, t_0 and dt' were determined for each plant. The instantaneous rates of stomatal opening (dg/dt, mol m^{-2} s^{-2}) across the entire range of t were then calculated by taking the derivative of Equation 1:

$$\frac{dg}{dt} = \frac{e^{(t_0+t)/dt'}\left(a_2 - a_1\right)}{\left(e^{t_0/dt'} + e^{t/dt'}\right)^2 dt'} \quad (2)$$

and the maximum rate of stomatal opening (dg/dt_{max}, mol m^{-2} s^{-2}) determined for each plant as dg/dt when $t = t_0$.

This procedure was repeated after converting g to a relative value, $g_{relative}$:

$$g_{relative} = \frac{g - g_{min(dawn)}}{g_{op} - g_{min(dawn)}}, \quad (3)$$

and the time taken to reach 50% of $g_{relative}$ (t_{50}, minutes) determined.

Stomatal morphology

A tissue sample was obtained halfway from the leaf tip to the base from each leaf that was analysed for gas exchange properties and stored in 70% ethanol. For all species except *B. littoralis*, stomata were concentrated within crypts on the abaxial surface. Stomata of *B. littoralis* also only occurred on the abaxial surface but no crypts were observed. The leaf epidermal surface of each species was also comprised of thickly intertwined trichomes. To obtain a clear view of stomata amidst these surface features, each sample was first rehydrated by rinsing under tap water then embedded in paraffin wax. Planar (through the epidermis) and transverse sections were then cut to 10 μm thickness with a rotary microtome (Leica model RM 2125, Leica Microsystems, Wetzlar, Germany). The sections were then positioned on slides that were dipped in 2% gelatin immediately prior to mounting. Slides were then placed in a coplin jar with filter paper soaked in formaldehyde to allow vapour fixation (of section to gelatin). The coplin jar was covered with a lid and the sections allowed to dry at room temperature for 12 hours. Sections were then stained in 0.1% aqueous

toluidine blue, examined under a compound light microscope and images captured with a digital camera.

Stomatal morphological parameters (guard cell length L (μm) and guard cell pair width W (μm)) were measured from images obtained from planar sections as the mean of 20 stomatal complexes (guard cell pairs) for each species. We report stomatal size (S) as the product of L and W (μm^2).

For each species stomatal density, i.e. number of stomata per unit epidermal area (D, mm^{-2}) was calculated from transverse sections. For each section, the number of stomata (n_s) intercepted by the microtome during cutting was counted along a known length of epidermis (l, μm, n = 12 lengths per species). The length of epidermis ranged from approximately 450 μm to 4400 μm. Assuming each transect captured an area of epidermis of width (w_e) approximately equal to the average of the length and width of a stoma, the stomatal density was calculated as $D = n_s/(l \times w_e)$.

RESULTS

The operating stomatal conductance g_{op} was positively correlated with $g_{min(dawn)}$ ($y = 0.844 – 0.562e^{-(x - 0.004)/0.024}$, $r^2 = 0.70$, Fig. 3A) and with $(dg/dt)_{max}$ (Fig. 3B, $y = -0.09 + 3.40x$, $r^2 = 0.71$, $P < 0.001$). Across species there was a three-fold variation in $(dg/dt)_{max}$, ranging from 0.07 mmol m^{-2} s^{-2} to 0.25 mmol m^{-2} s^{-2}. $g_{min(dawn)}$ was also positively correlated with $(dg/dt)_{max}$ (Fig 3C, $y = 5.08 \times 10^{-6}e^{(x/0.03)} + 0.01$, $r^2 = 0.78$). These results indicate that higher maximum and minimum stomatal conductance is linked to faster absolute rates of response of stomatal stomatal conductance to leaf irradiance.

Stomatal size (S) was negatively correlated with $(dg/dt)_{max}$ across species (Fig. 4A, $y = 15877.84 \times e^{(-x/0.03)} + 340.52$, $r^2 = 0.88$, $P < 0.01$) and stomatal density D was positively correlated with $(dg/dt)_{max}$ (Fig. 4B, $y = 77.43 + 1643.06x$, $r^2 = 0.71$, $P < 0.05$), indicating that leaves with smaller and more numerous stomata exhibit faster absolute rates of response of stomatal conductance to water vapour. The positive relationship between t_{50} and S (Fig. 4C, $y = 16.63 + 0.05x$, $r^2 = 0.34$, $P < 0.05$) further indicates that smaller stomata exhibited a faster response in relative terms.

Stomatal opening in response to a step increase in light followed a similar pattern in all species, resembling the typical dynamic response of a second order

dynamic system with near-critical damping (Fig 5A-E). For each species the stomatal opening phase was accompanied by an increase in CO_2 assimilation rate (A) to a maximum steady-state value (A_{op}), although A_{op} was established prior to g_{op} (Fig 5F-J).

Although g_{op} varied by about five fold across species, $g_{min(dawn)}$ varied by 15 fold (Table 2.). Across the five species, there was well over a two-fold range between highest and lowest mean species g_{op} measured under controlled laboratory conditions. The mean absolute minimum stomatal conductance $g_{min(abs)}$ ranged from 6.0 to 20 mmol m^{-2} s^{-1}, which compares favourably to the range of minimum stomatal conductance reported for deciduous and evergreen plants using leaf drying curves (1.0 to 20 mmol m^{-2} s^{-1}) (Burghardt and Riederer, 2003).

Over the dynamic range of stomatal opening, CO_2 assimilation rate increased with stomatal conductance in the usual saturating fashion (Fig. 6A). Steady-state instantaneous water use-efficiency (WUE_i), defined as A_{op}/E_{op} at 1 kPa VPD (see the controlled, standardised environmental conditions in Methods) ranged from 2.5 to 6.5 mmol mol^{-1} and all of the species reached a peak in WUE_i when A was about 5 μmol m^{-2} s^{-1} (Fig. 6B). *B. attenuata* and *B. menzeisii* had the highest WUE_i and *B. littoralis* had the lowest WUE_i (Fig. 6B). Also, WUE_i was negatively correlated with g_{op} (Fig. 6C; $y = 6.49 - 4.51x$; $r^2 = 0.52$, $P < 0.001$).

The maximum rate of carboxylation (Vc_{max}) ranged from 23.90 μmol m^{-2} s^{-1} to 47.11 μmol m^{-2} s^{-1} and the light saturated rate of electron transport (J_{max}) ranged from 64.2 μmol m^{-2} s^{-1} to 131 μmol m^{-2} s^{-1}. The average value of Vc_{max} and J_{max} was 37.22 ± 1.47 μmol m^{-2} s^{-1} and 103.74 ± 4.24 μmol m^{-2} s^{-1} respectively. This is lower than the average values reported by (Wullschleger SD, 1993) for sclerophyllous shrubs (53 ± 15 μmol m^{-2} s^{-1} and 122 ± 31 μmol m^{-2} s^{-1} for Vc_{max} and J_{max} respectively), but is similar to the values for temperate forest hardwoods (47 ± 33 μmol m^{-2} s^{-1} and 104 ± 67 μmol m^{-2} s^{-1} for Vc_{max} and J_{max} respectively). Across individual plants $A_{(op)}$ (defined here as the maximum operating CO_2 assimilation rate under standard conditions, as distinct from the maximum ribulose bisphosphate regeneration limited rate induced under elevated CO_2 concentration) was positively correlated with Vc_{max} (Fig. 7A) and J_{max} (Fig. 7B) ($y = 0.47x - 1.39$, $r^2 = 0.81$, $P < 0.001$ for $A_{op(max)}$ versus Vc_{max} and $y = 0.14x + 1.14$, $r^2 = 0.64$ $P < 0.001$ for $A_{(op)max}$ versus J_{max}). There was no apparent species grouping within either correlation.

Stomatal closure in response to darkening of leaves followed a similar pattern across species, but the minimum steady conductance during this midday darkening of leaves, $g_{min(day)}$, was considerably higher than $g_{min(dawn)}$ (Fig. 8). The average percentage decline in g after midday darkening, with respect to the illuminated steady-state conductance (g_{op}), was 59.23, 61.80, 64.36, 65.57 and 86.08 for *B. menziesii*, *B. prionotes*, *B. ilicifolia*, *B. attenuata*, and *B. littoralis* respectively. After excising leaves, a further decline in g was noted. The average percentage decline in g with leaf excision, relative to $g_{min(day)}$, was 95.00, 93.28, 95.20, 94.87 and 79.93 for *B. attenuata*, *B. menziesii*, *B. ilicifolia*, *B. prionotes* and *B. littoralis* respectively. On this occasion *B. littoralis*, the species restricted to sites with high soil moisture, showed the least relative decline in g.

DISCUSSION

In support of hypotheses (i) and (ii), g_{op} correlated with $g_{min(dawn)}$ and with the maximum rate of stomatal response to light, $(dg/dt)_{max}$ (Fig. 3A, 3B). The results suggest that the day and night-time stomatal conductances are positively correlated across these *Banksia* species and that a functional connection exists between these traits and the dynamic behaviour of stomata. Enhanced dynamic response with higher operational stomatal conductcance has implications for improved long-term water-use efficiency and lower risk of disruption of the leaf hydraulic system.

The positive correlation between g_{op} and $g_{min(dawn)}$ (Fig. 3A) suggests that there is a trade-off in which leaves built for higher rates of leaf gas exchange maintain higher stomatal conductance at night. The positive correlation also between g_{op} and $(dg/dt)_{max}$ (Fig. 3B) suggests that the water losses due to the accompanying elevated night-time stomatal conductance and, consequently, the elevated night-time transpiration rates are offset by better dynamic control of stomata during the day. The role of night-time stomatal conductance remains elusive and the mechanism of its control is poorly understood (Barbour and Buckley, 2007). However, the scaling relationships identified in our study provide important mechanistic foundations for predicting the dynamic range of stomatal control and for improved modelling of stomatal control through day-night cycles.

Higher g_{op}, faster $(dg/dt)_{max}$ and shorter t_{50} were associated with smaller and more numerous stomata (Fig. 4A-C). Investment in stomatal infrastructure to

facilitate high gas exchange capacity is constrained by the availability of space on the leaf surface and the total metabolic energy required to actively regulate stomatal pore size in a given number of stomata (Franks and Farquhar, 2007; Franks *et al*., 2009). Our study suggests that the inherently faster stomatal response of leaves with high g_{op} and smaller stomata could provide enhanced water balance in dynamic light environments in addition to the higher assimilation rates accompanying high g_{op}. However, the interaction between the dynamic response of stomata and the frequency of light fluctuations is complex, with frequency dramatically influencing the average stomatal response (Cardon *et al*., 1994).

Despite the advantages of faster stomatal response (i.e. compared to leaves with the same g_{op} but slower stomatal response), greater overall water-use efficiency may still be more strongly associated with lower g_{op}, as suggested by the negative correlation between WUE_i and g_{op} across species (Fig 6C). However, the faster response times associated with higher g_{op} (Fig 3B, Fig 4C) help to compensate for this. WUE_i trended towards higher values in species that occur naturally in areas with a large depth to groundwater (Table 1) and therefore higher probability of water deficit. Assuming these qualities are genetically conserved and the observed differences translate qualitatively to these species in their natural environment, the results help to explain why the species with higher photosynthetic capacity prefer damp habitats while those with lower capacity occupy seasonally dry habitats (Fig. 2). Similarly, Anderson *et al*. (1996) showed that the water-use efficiency of commonly grown *Eucalyptus* species correlated negatively with the rainfall of their respective native habitat, suggesting genetic conservation of gas exchange traits that have been optimised to local conditions. Faster stomatal response improves water-use efficiency in environments with fluctuating light and evaporative demand, so higher $(dg/dt)_{max}$ associated with higher g_{op} will help to counteract reduced WUEi in leaves with high g_{op}.

The correlation between g_{op} and $(dg/dt)_{max}$ is consistent with selection for a stomatal control mechanism that minimizes exposure to excessive water potential gradients. With increasing g_{op} the plant is more exposed to potentially damaging water potential gradients arising from sudden changes in evaporation potential. Faster stomatal closure in response to these changes will reduce the risks associated with such exposure, including formation of air embolisms in the xylem. Stomatal response to light and VPD (or transpiration rate) have similar kinetics (Grantz and Zeiger,

1986), so it may be useful to compare species on the basis of them having generally 'faster' or 'slower' stomatal mechanisms. In Fig. 9 we illustrate the value of faster response times for plants with higher g_{op}. The simulations use the data and model in Franks (2006) for plants with different gas exchange and hydraulic capacities. It is shown that, for a step increase in VPD from 1 to 1.5 kPa, plants operating with higher g_{op} at 1 kPa VPD are exposed to higher leaf water potential gradients ($\Delta\Psi_{leaf}$) immediately after the change, and may therefore benefit from a faster rate of reduction of stomatal conductance to the new steady rate at 1.5 kPa VPD.

Conclusions

Although several studies have demonstrated scaling of stomatal conductance with static indictors of plant gas exchange capacity (Wong et al.1979; Field and Mooney, 1986; Meinzer, 2003), our results show scaling with a dynamic performance characteristic, $(dg/dt)_{max}$, and this dynamic attribute also scaled with stomatal size and stomatal density. Maximum daytime operating stomatal conductance, g_{op}, and pre-dawn minimum stomatal conductance, $g_{min(dawn)}$, were positively correlated with the rate of stomatal response to light. Leaves with higher g_{op} have lower instantaneous water-use efficiency and are exposed to larger transient water potential gradients. Faster stomatal response times in such leaves may improve long-term water-use efficiency and reduce exposure to transient water potential gradients. Smaller stomata with faster dynamic characteristics may therefore be integral to selection for high stomatal conductances accompanying higher photosynthetic capacity. This principle may also be applied in the selection for plants with improved agricultural qualities.

ACKNOWLEDGMENTS

We thank Robyn Loomes and Muriel Davies for maintaining the glasshouse and Gordon Thomson for assistance with histology. We are also grateful for helpful comments from Daniel Mendham. This project was supported by the Australian Research Council (grant number LP-0669240).

REFERENCES

Aasama K, Sõber A, Rahi M. (2001) Leaf anatomical characteristics associated with shoot hydraulic conductance, stomatal conductance and stomatal sensitivity to changes of leaf water status in temperate deciduous trees. *Australian Journal of Plant Physiology* **28,** 765-774.

Anderson JE, Williams J, Kriedemann PE, Austin MP, Farquhar GD. 1996. Correlations between carbon isotope discrimination and climate of native habitats for diverse eucalypt taxa growing in a common garden. *Australian Journal of Plant Physiology* **23**, 311-320.

Assmann SM, Grantz DA. 1990. Stomatal response to humidity in sugarcane and soybean: effect of vapour pressure difference on the kinetics of the blue light response. *Plant, Cell and Environment* **13**, 163-169.

Barbour MM, Cernusak LA, Whitehead D, Griffin KL, Turnbull MH, Tissue DT, Farquhar GD. 2005. Nocturnal stomatal conductance and implications for modelling delta $\delta^{18}O$ of leaf-respired CO_2 in temperate tree species. *Functional Plant Biology* **32**, 1107-1121.

Barbour MM, Buckley TN. 2007. The stomatal response to evaporative demand persists at night in *Ricinus communis* plants with high nocturnal conductance. *Plant, Cell and Environment* **30**, 711-721.

Benyon RG. 1999. Nighttime water use in an irrigated *Eucalyptus grandis* plantation. *Tree Physiology* **19**, 853-859.

Brodribb TJ, Field TS, Jordan GS. 2007. Leaf maximum photosynthetic rate and venation are linked by hydraulics. *Plant Physiology* **144**, 1890-1898.

Brodribb TJ, McAdam S. A. M., Jordan GJ, Field TS. 2009. Evolution of stomatal responsiveness to CO_2 and optimisation of water-use efficiency among land plants. *New Phytologist*. 183, 839-847.

Bucci SJ, Goldstein G, Meinzer FC, Franco AC, Campanello P, Scholz FG. 2005. Mechanisms contributing to seasonal homeostasis of minimum leaf water potential and predawn disequilibrium between soil and plant water potential in neotropical savanna trees. *Trees-Structure and Function* **19**, 296-304.

Burghardt M, Riederer M. 2003. Ecophysiological relevance of cuticular transpiration of deciduous and evergreen plants in relation to stomatal closure and leaf water potential. *Journal of Experimental Botany* **54**, 1941-1949.

Caird MA, Richards JH, Donovan LA. 2007. Nighttime stomatal conductance and transpiration in C_3 and C_4 plants. *Plant Physiology* **143**, 4-10.

Cowan IR. 1977. Stomatal behaviour and environment. *Advances in Botanical Research* **4**, 117-228.

Daley MJ, Phillips NG. 2006. Interspecific variation in nighttime transpiration and stomatal conductance in a mixed New England deciduous forest. *Tree Physiology* **26**, 411-419.

Dawson TE, Pate JS. 1996. Seasonal water uptake and movement in the root systems of Australian phreatophytic plants of dimorphic root morphology: A stable isotope investigation. *Oecologia* **107**, 13-20.

Dawson TE, Burgess SSO, Tu KP, Oliveira RS, Santiago LS, Fisher JB, Simonin KA, Ambrose AR. 2007. Nighttime transpiration in woody plants from contrasting ecosystems. *Tree Physiology* **27**, 561-575.

Ehrler WL. 1971. Periodic nocturnal stomatal opening of citrus in a steady environment. *Physiologia Plantarum* **25**, 488-&.

Farquhar GD, Caemmerer SV, Berry JA. 1980. A biochemical model of photosynthetic CO_2 assimilation in leaves of C_3 species. *Planta* **149**, 78-90.
Farquhar GD, Schulze ED, Kuppers M. 1980. Responses to humidity by stomata of *Nicotina glauca* L. and *Corylus avellana* L. are consistent with the optimization of carbon dioxide uptake with respect to water loss. *Australian Journal of Plant Physiology* **7**, 315-327.
Field CB, Mooney HA. 1986. The photosynthetic-nitrogen relationship in wild plants. In: Givnish TJ, ed. *On the economy of plant form and function*. Cambridge: Cambridge University Press, pp. 22-55.
Franks PJ. 2006. Higher rates of leaf gas exchange are associated with higher leaf hydrodynamic pressure gradients. *Plant Cell and Environment* **29**, 584-592.
Franks PJ, Farquhar GD. 1999. A relationship between humidity response, growth form and photosynthetic operating point in C_3 plants. *Plant, Cell and Environment* **22**, 1337-1349.
Franks PJ, Farquhar GD. 2007. The mechanical diversity of stomata and its significance in gas-exchange control. *Plant Physiology* **143**, 78-87.
Franks PJ, Beerling DJ. 2009. CO_2-forced evolution of plant gas exchange capacity and water-use efficiency over the Phanerozoic. *Geobiology* **7**, 227-236.
Franks PJ, Drake PL, Beerling DJ. 2009. Plasticity in maximum stomatal conductance constrained by negative correlation between stomatal size and density: an analysis using *Eucalyptus globulus*. *Plant Cell and Environment* **32**, 1737-1748.
Grantz DA, Zeiger E. 1986. Stomatal responses to light and leaf-air water vapour pressure differences show similar kinetics in sugarcane and soybean. *Plant Physiology* **81**, 865-868.
Groom PK, Froend RH, Mattiske EM. 2001. Long-term changes in vigour and distribution of *Banksia* and *Melaleuca* overstorey species on the Swan Coastal Plain. *Journal of the Royal Society of Western Australia* **84**, 63-69.
Groom PK. 2002. Seedling water stress response of two sandplain Banksia species differing in ability to tolerate drought. *Journal of Mediterranean Ecology* **3**, 3-9.
Groom PK. 2004. Seedling growth and physiological response of two sandplain *Banksia* species differing in flood tolerance. *Journal of the Royal Society of Western Australia* **87**, 115-121.
Harley PC, Thomas RB, Reynolds JF, Strain BR. 1992. Modelling photosynthesis of cotton grown in elevated CO_2. *Plant, Cell and Environment* **15**, 271-282.
Hetherington AM, Woodward FI. 2003. The role of stomata in sensing and driving environmental change. *Nature* **424**, 901-908.
Hinckley TM, Duhme F, Hinckley AR, Richter H. 1980. Water relations of drought-hardy shrubs: Osmotic potential and stomatal reactivity. *Plant Cell and Environment* **3**, 131-140.
Jones HG. 1992. *Plants and Microclimate*. Cambridge: Cambridge University Press.
Körner C. 1995. Leaf diffusive conductances in the major vegetation types of the globe. In: Schulz E-D, Caldwell MM, eds. *Ecophysiology of Photosynthesis*. Berlin: Springer-Verlag, 463-490.
Lam A, Froend RH, Downes S, Loomes R. 2004. Water availability and plant response: Identifying the water requirements of *Banksia* woodland on the Gnangara Groundwater Mound. A report to the Water Corporation of Western Australia.
McDowell N, Pockman WT, Allen CD, Breshears DD, Cobb N, Kolb T, Plaut J, Sperry J, West A, Williams DG, Yepez EA. 2008. Mechanisms of plant survival and mortality during drought: why do some plants survive while others succumb to drought? *New Phytologist* **178**, 719-739.

Meinzer FC. 2003. Functional convergence in plant responses to the environment. *Oecologia* **134**, 1-11.
Novick KA, Oren R, Stoy PC, Siqueira MBS, Katul GG. 2009. Nocturnal evapotranspiration in eddy-covariance records from three co-located ecosystems in the Southeastern US: Implications for annual fluxes. *Agricultural and Forest Meteorology* **149**, 1491-1504.
Pate JS, Jeschke WD, Aylward MJ. 1995. Hydraulic Architecture and Xylem Structure of the Dimorphic Root Systems of South-West Australian Species of Proteaceae. *Journal of Experimental Botany* **46**, 907-915.
Schulze ED, Kelliher FM, Körner C, Lloyd J, Leuning R. 1994. Relationships among maximum stomatal conductance, ecosystem surface conductance, carbon assimilation rate, and plant nitrogen nutrition- A global ecology scaling exercise. *Annual Review of Ecology and Systematics* **25**, 629-660.
Sharkey TD. 1985. Photosynthesis in intact leaves of C_3 plants: physics, physiology and rate limitations. *The Botanical Review* **51**, 53-105.
Snyder KA, Richards JH, Donovan LA. 2003. Night-time conductance in C_3 and C_4 species: do plants lose water at night? *Journal of Experimental Botany* **54**, 861-865.
Vico G, Manzoni S, Palmroth S, Katul G. 2011. Effects of stomatal delays on the economics of leaf gas exchange under intermittent light regimes. *New Phytologist* **192**, 640-652.
von Caemmerer S, Farquhar GD. 1981. Some relationships between the biochemistry of photosynthesis and the gas exchange of leaves. *Planta* **153**, 376-387.
Wong SC, Cowan IR, Farquhar GD. 1979. Stomatal conductance correlates with photosynthetic capacity. *Nature* **282**, 424-426.
Wullschleger SD. 1993. Biochemical limitations to carbon assimilation in C_3 plants - a retrospective analysis of the A/c_i curves from 109 Species. *Journal of Experimental Botany* **44**, 907-920.
Zencich SJ, Froend RH, Turner JV, Gailitis V. 2002. Influence of groundwater depth on the seasonal water sources of water accessed by *Banksia* tree species on a shallow, sandy coastal aquifer. *Oecologia* **131**, 8-19.

Table 1. Approximate range in groundwater depth of the study species

Species	Approximate range of groundwater depth (m)	Source
Banksia attenuata	3 to > 30	Zencich *et al*., 2002; Lam *et al*., 2004
Banksia menziesii	3 to > 30	Lam *et al*., 2004)
Banksia prionotes	1.5 to 10	Dawson and Pate, 1996; Pate *et al*., 1995
Banksia ilicifolia	< 10	Groom *et al*., 2001; Zencich *et al*., 2002
Banksia littoralis	< 5	Groom *et al*., 2001

Table 2. Comparison of stomatal conductances to water vapour (mmol m^{-2} s^{-1}) in the five *Banksia* species studied: $g_{min(dawn)}$, prior to morning light exposure; g_{op}, at full stomatal opening under ideal conditions; $g_{min(day)}$, following closure in response to leaf darkening at midday; $g_{min(abs)}$, after leaf excision. Numbers are means with standards error in brackets.

Species	$g_{min(dawn)}$	g_{op}	$g_{min(day)}$	$g_{min(abs)}$
B. attenuata	9.42 (1.9)	345 (20)	120 (19)	5.7 (0.8)
B. menziesii	6.03 (0.7)	356 (34)	135 (25)	9.5 (0.8)
B. illicifolia	12.4 (1.8)	421 (32)	143 (23)	8.5 (2.7)
B. prionotes	12.9 (1.1)	469 (4)	171 (20)	8.8 (0.7)
B. littoralis	44.0 (2.9)	761 (19)	95 (4)	20 (0.7)

FIGURE LEGENDS

Figure 1. The different phases of stomatal conductance examined in this study: g_{min}, steady state stomatal conductance in darkness, either at dawn ($g_{min(dawn)}$) or after suddenly induced darkness ($g_{min(day)}$); $(dg/dt)_{max}$, the maximum rate of change of g during light-induced stomatal opening; g_{op}, steady state operating stomatal conductance under standardised ideal conditions (see Methods); t_{50}, time taken to reach 50% of the range between g_{min} and g_{op}; $g_{min(abs)}$; the absolute minimum steady-state stomatal conductance after leaf excision, assumed to result from zero turgor in stomatal guard cells.

Figure 2. Idealized distribution of *Banksia* species on the Gnangara Groundwater Mound with respect to depth to groundwater (see Table 1) and unsaturated soil volume. *Banksia littoralis* only occurs in association with watercourses and wetland habitats and are excluded from dune crests occupied by *Banksia attenuata* and *Banksia menzeisii*. Accordingly, *B. littoralis* has a highly restricted geographical distribution, while *B. attenuata* and *B. menzeisii* have a more extensive geographical distribution encompassing several hydrological habitats. Adapted from Lam *et al*., 2004. Inset: Illustrating the range of leaf size and shape across the study species.

Figure 3. Relationship between g_{op}, $g_{min(dawn)}$ and $(dg/dt)_{max}$. (A) Across individuals, g_{op} was positively correlated with $g_{min(dawn)}$. Each point represents the mean ± S.E. of $n = 6$ consecutive steady-state records for an individual plant. The maximum rate of stomatal opening $(dg/dt)_{max}$ was positively correlated with maximum steady-state stomatal conductance, g_{op} (B) and minimum stomatal conductance induced by darkness, $g_{min(day)}$ (C).

Figure 4. Smaller, faster stomata. The maximum rate of stomatal opening $(dg/dt)_{max}$ was negatively correlated with maximum stomatal size, S (panel A) and positively correlated with stomtal density D, (panel B). The time to reach 50% of the range between $g_{min(dawn)}$ and g_{op} (t_{50}) was positively correlated with stomatal size (panel C).

Figure 5. Time-series of stomatal opening and CO_2 assimilation rate in response to light. Each point is the mean ± S.E. stomatal conductance (g, panels A-E) and assimilation rate (A, panels F-J) measured at discrete time intervals ($n = 4$ plants per species). The letter "I" in each graph indicates the start of the illumination phase, when leaves were exposed to a PAR of 1500 μmol m^{-2} s^{-1}. Prior to this point leaves were darkened (PAR = 0 μmol m^{-2} s^{-1}).

Figure 6. Relationship between CO_2 assimilation rate, stomatal conductance and instantaneous water use efficiency. Panel (A), instantaneous CO_2 assimilation rate A versus instantaneous stomatal conductance g; panel (B), instantaneous water-use efficiency WUE_i versus g. Note the peak in WUEi at around the same A for all species (approximately 5 μmol m^{-2} s^{-1}); panel (C), negative correlation between WUEi and steady state operating stomatal conductance, g_{op}.

Figure 7. The maximum (operating) photosynthetic rate A_{op} was positively correlated with the maximum rate of carboxylation, Vc_{max} (panel A) and the light saturated rate of electron transport, J_{max} (panel B).

Figure 8. Incomplete stomatal closure in the dark. Following a sudden transition from 1500 to 0 PAR (indicated by the arrow labelled "dark"), stomatal conductance (g) declined to a steady state minimum ($g_{min(day)}$, see Fig. 1). Further reduction in g occurred after leaf excision (indicated by the arrow), reaching the absolute minimum conductance ($g_{min(abs)}$) after desiccation induced the complete loss of guard cell turgor. Panels A-E show the time series of g for each species (mean ± S.E., n = 4 plants per species).

Figure 9. Simulations based on the data and model in (Franks PJ, 2006) show that following an increase in evaporative demand (leaf-to-air vapour pressure difference, VPD), plants that operate with higher stomtatal conductance g_{op} are exposed to larger water potential gradients (shown here for leaves, $\Delta\Psi_{leaf}$; A), even though they have inherently larger maximum leaf hydraulic conductance $k_{leaf(max)}$ (B). For illustrative purposes two operating stomatal conductances are contrasted with one another (0.10 and 0.20 mol m^{-2} s^{-1} at 1 kPa VPD), with their initial and final values indicated by the start and end point (respectively) of the arrows. Faster response time reduces the duration of exposure to excessive water potential gradients.

Figure 1

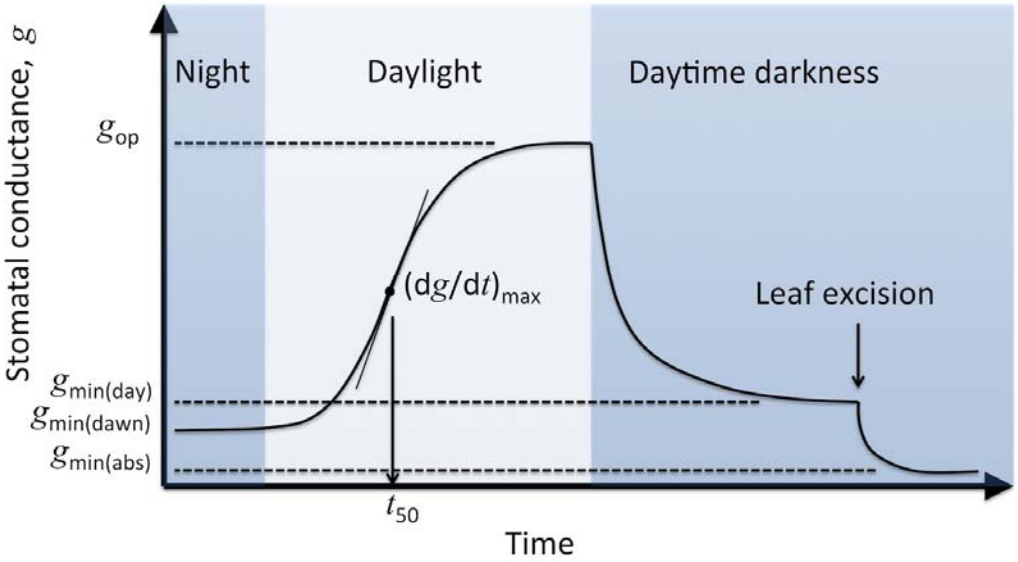
Stomatal conductance, g
Night
Daylight
Daytime darkness
g_{op}
$(dg/dt)_{max}$
Leaf excision
$g_{min(day)}$
$g_{min(dawn)}$
$g_{min(abs)}$
t_{50}
Time

Figure 2

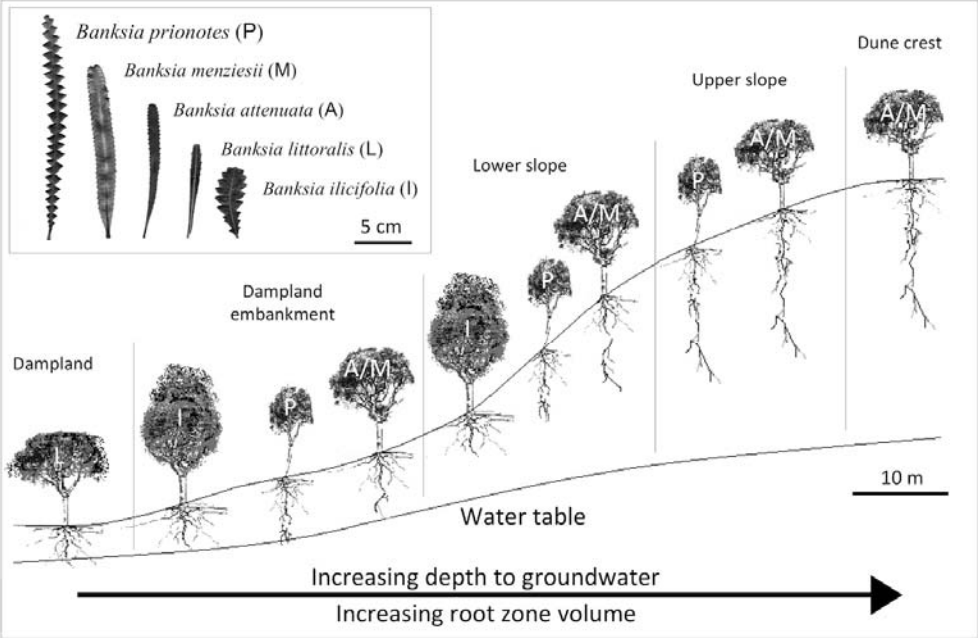
Banksia prionotes (P)
Banksia menziesii (M)
Banksia attenuata (A)
Banksia littoralis (L)
Banksia ilicifolia (I)
5 cm
Dune crest
Upper slope
Lower slope
Dampland embankment
Dampland
A/M
P
I
L
10 m
Water table
Increasing depth to groundwater
Increasing root zone volume

Figure 3

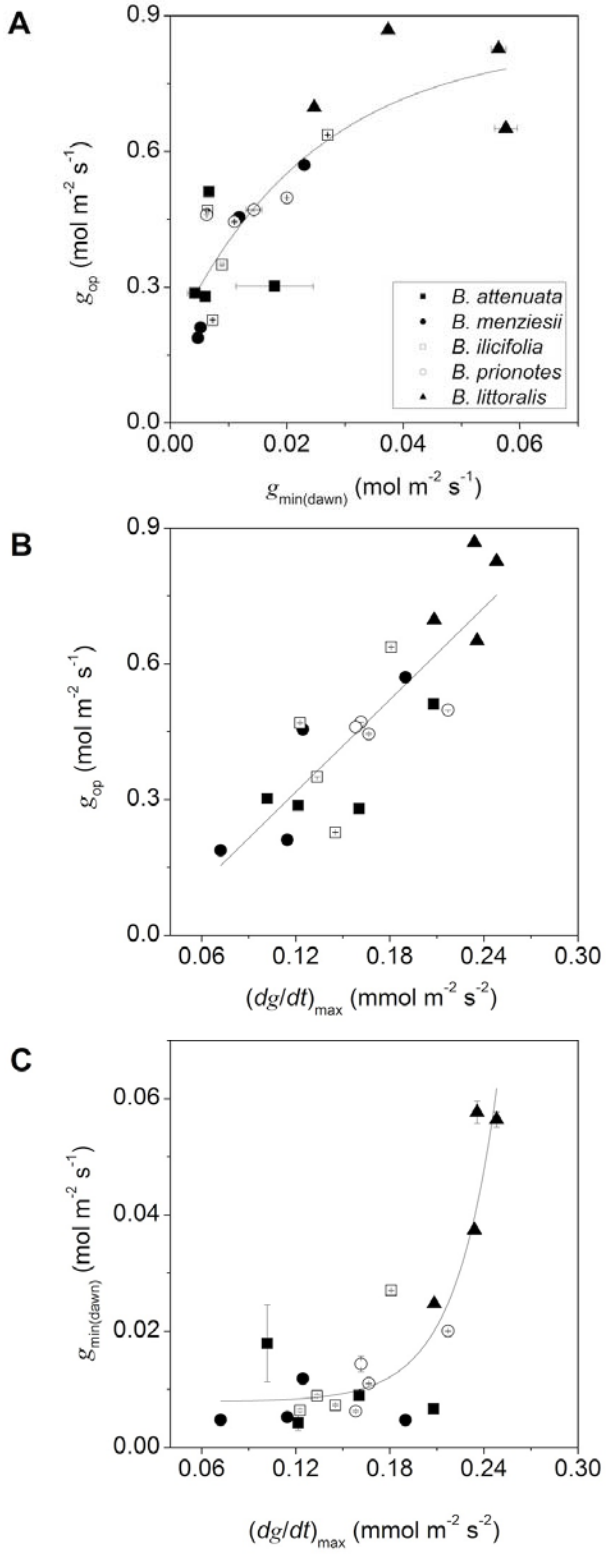
A
0.9
0.6
0.3
0.0
0.00
0.02
0.04
0.06
g_{op} (mol m^{-2} s^{-1})
$g_{min(dawn)}$ (mol m^{-2} s^{-1})
B. attenuata
B. menziesii
B. ilicifolia
B. prionotes
B. littoralis
B
0.9
0.6
0.3
0.0
0.06
0.12
0.18
0.24
0.30
g_{op} (mol m^{-2} s^{-1})
$(dg/dt)_{max}$ (mmol m^{-2} s^{-2})
C
0.06
0.04
0.02
0.00
0.06
0.12
0.18
0.24
0.30
$g_{min(dawn)}$ (mol m^{-2} s^{-1})
$(dg/dt)_{max}$ (mmol m^{-2} s^{-2})

Figure 4

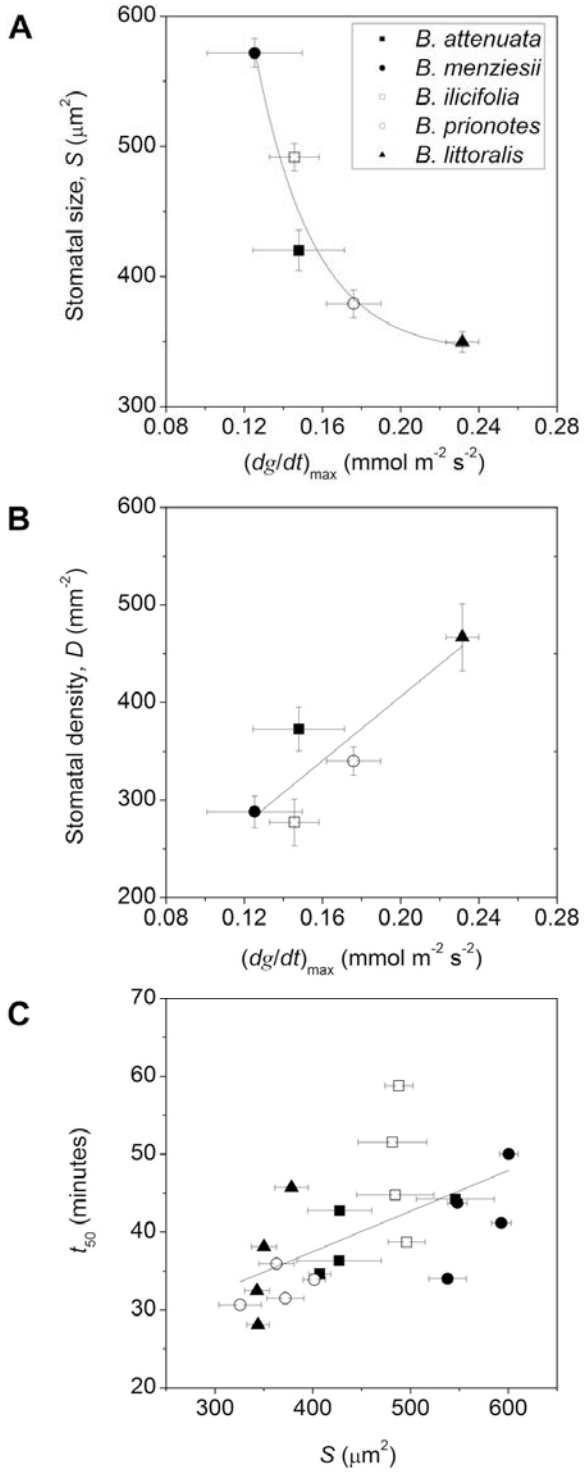
A
B. attenuata
B. menziesii
B. ilicifolia
B. prionotes
B. littoralis
Stomatal size, S (μm²)
600
500
400
300
0.08
0.12
0.16
0.20
0.24
0.28
(dg/dt)max (mmol m-2 s-2)
B
Stomatal density, D (mm-2)
600
500
400
300
200
0.08
0.12
0.16
0.20
0.24
0.28
(dg/dt)max (mmol m-2 s-2)
C
t50 (minutes)
70
60
50
40
30
20
300
400
500
600
S (μm²)

Figure 5

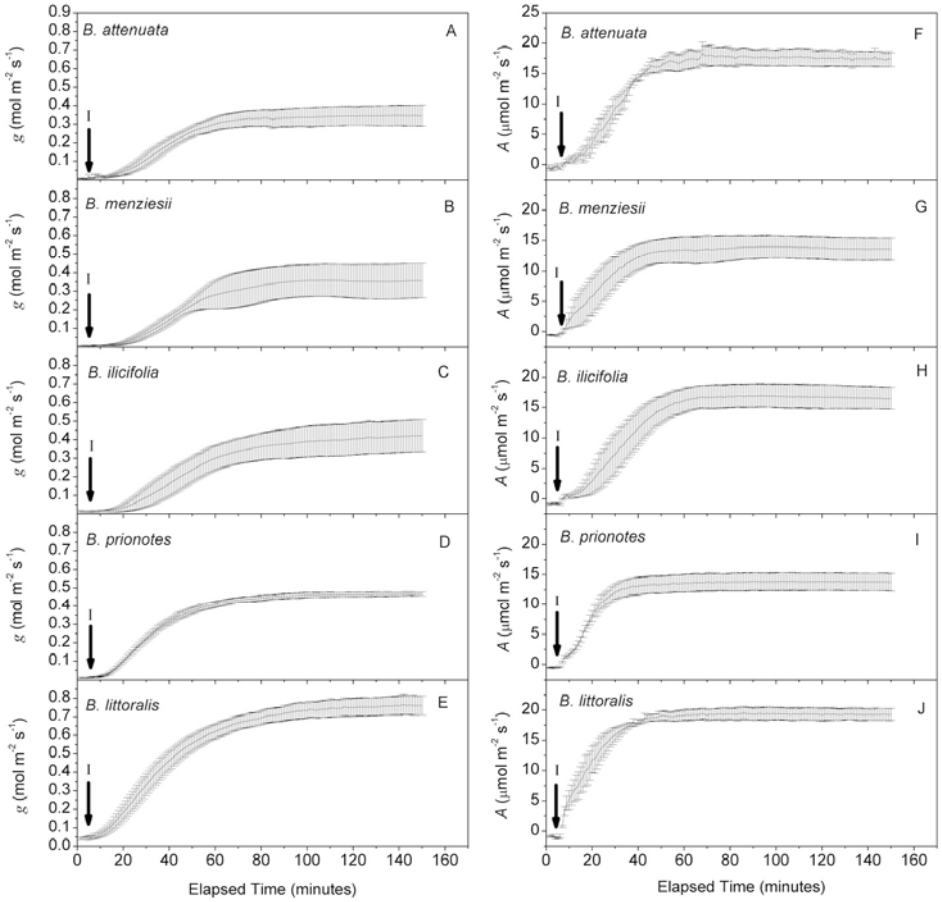
B. attenuata
A
B. menziesii
B
B. ilicifolia
C
B. prionotes
D
B. littoralis
E
B. attenuata
F
B. menziesii
G
B. ilicifolia
H
B. prionotes
I
B. littoralis
J
I
g (mol m-2 s-1)
A (µmol m-2 s-1)
Elapsed Time (minutes)

Figure 6

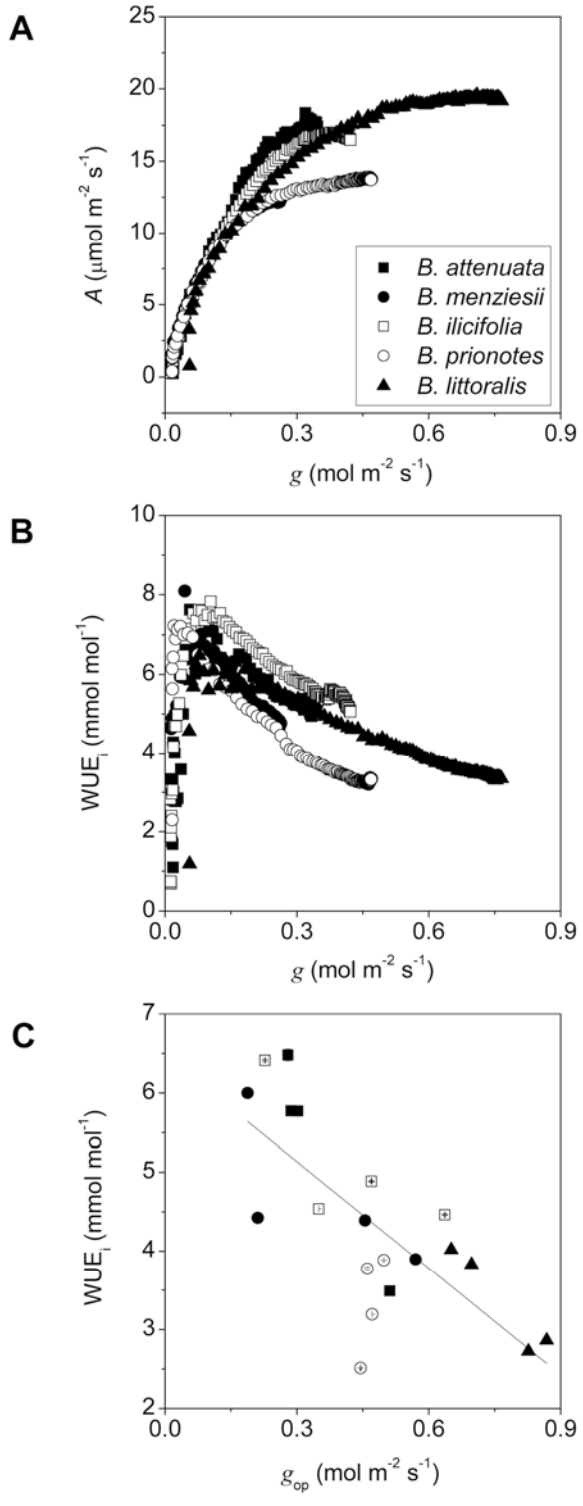
A
25
20
15
10
5
0
A (μmol m-2 s-1)
B. attenuata
B. menziesii
B. ilicifolia
B. prionotes
B. littoralis
0.0
0.3
0.6
0.9
g (mol m-2 s-1)
B
10
8
6
4
2
0
WUEi (mmol mol-1)
0.0
0.3
0.6
0.9
g (mol m-2 s-1)
C
7
6
5
4
3
2
WUEi (mmol mol-1)
0.0
0.3
0.6
0.9
gop (mol m-2 s-1)

Figure 7

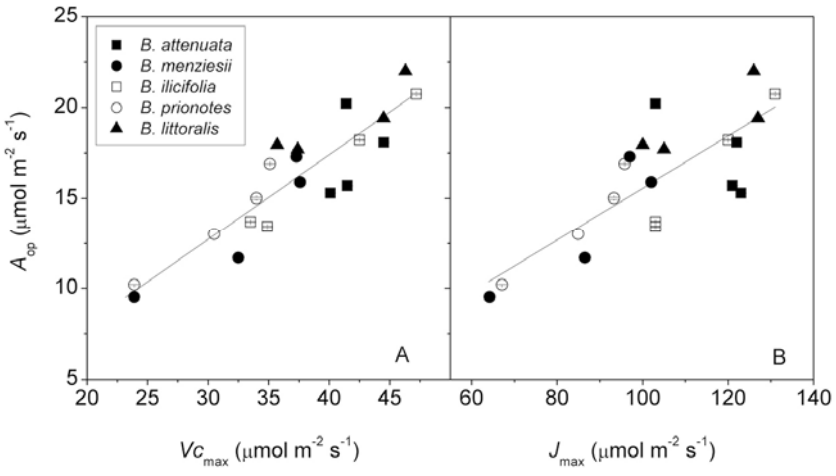
B. attenuata
B. menziesii
B. ilicifolia
B. prionotes
B. littoralis
A
B
A_{op} (μmol m^{-2} s^{-1})
Vc_{max} (μmol m^{-2} s^{-1})
J_{max} (μmol m^{-2} s^{-1})

Figure 8

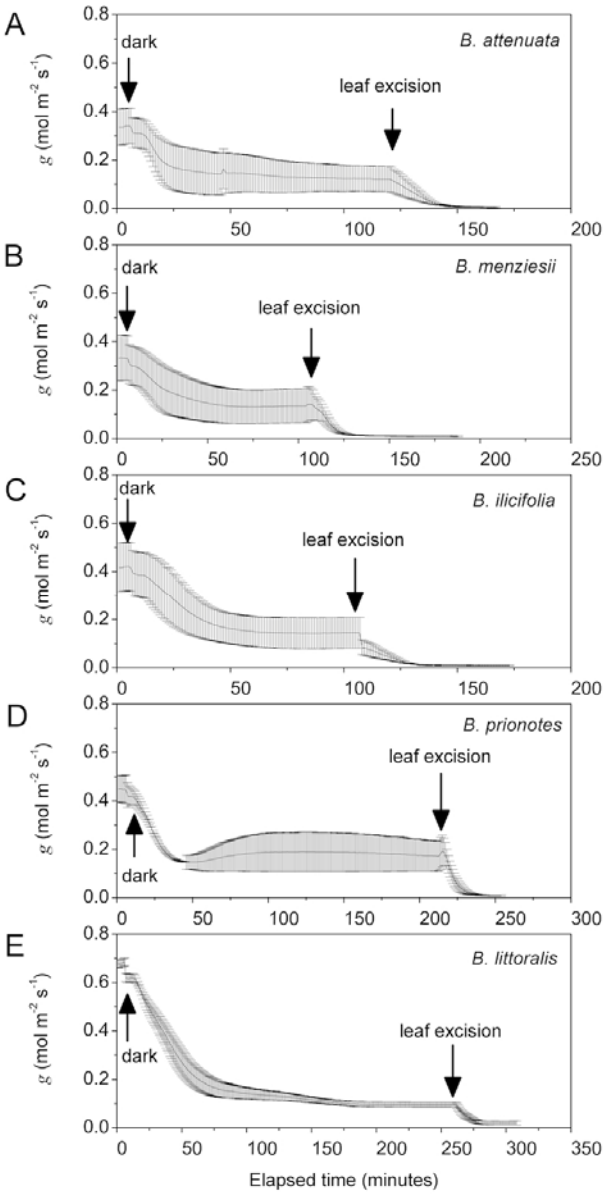
A
B. attenuata
dark
leaf excision
B
B. menziesii
dark
leaf excision
C
B. ilicifolia
dark
leaf excision
D
B. prionotes
leaf excision
dark
E
B. littoralis
dark
leaf excision
g (mol m-2 s-1)
Elapsed time (minutes)

Figure 9

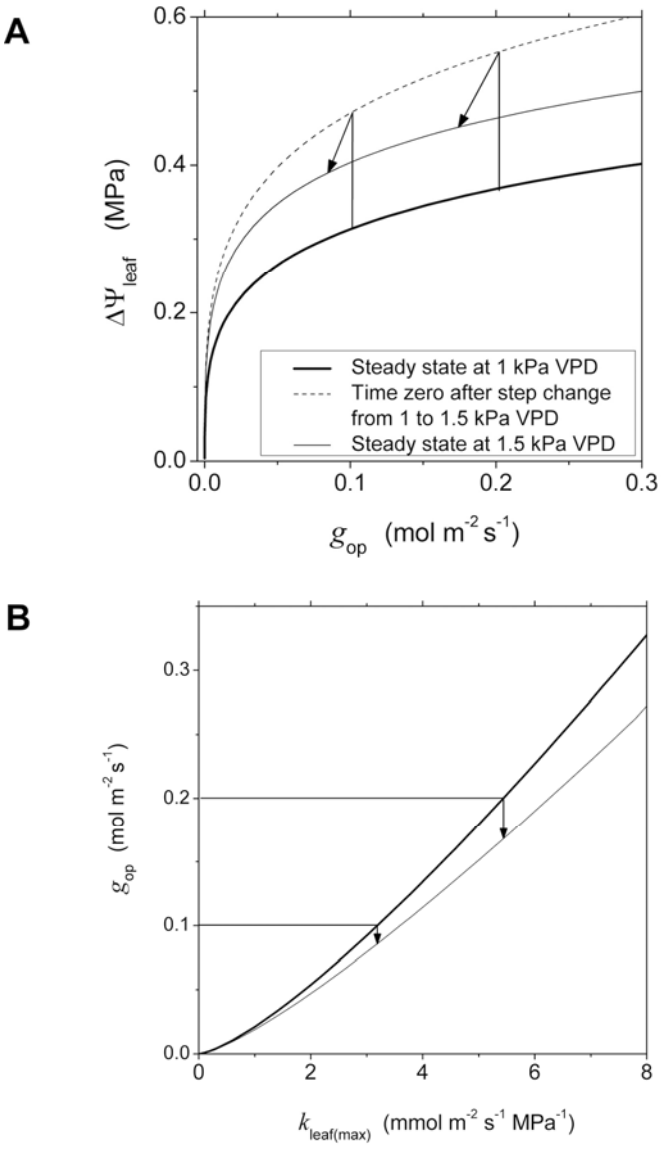
A
0.6
0.4
0.2
0.0
$\Delta\Psi_{leaf}$ (MPa)
Steady state at 1 kPa VPD
Time zero after step change from 1 to 1.5 kPa VPD
Steady state at 1.5 kPa VPD
0.0
0.1
0.2
0.3
g_{op} (mol m^{-2} s^{-1})
B
0.3
0.2
0.1
0.0
g_{op} (mol m^{-2} s^{-1})
0
2
4
6
8
$k_{leaf(max)}$ (mmol m^{-2} s^{-1} MPa^{-1})